Development 139, 2566-2575 (2012) doi:10.1242/dev.078618

DEVELOPMENT-RELATED PcG TARGET IN THE APEX 4 controls leaf margin architecture in *Arabidopsis thaliana*

Julia Engelhorn[1], Julia J. Reimer[1], Iris Leuz[1], Ulrike Göbel[2], Bruno Huettel[3], Sara Farrona[1] and Franziska Turck[1,*]

SUMMARY

In a reverse genetics screen based on a group of genes enriched for development-related Polycomb group targets in the apex (DPAs), we isolated *DPA4* as a novel regulator of leaf margin shape. T-DNA insertion lines in the *DPA4* locus display enhanced leaf margin serrations and enlarged petals, whereas overexpression of *DPA4* results in smooth margins. *DPA4* encodes a putative RAV (Related to ABI3/VP1) transcriptional repressor and is expressed in the lateral organ boundary region and in the sinus of leaf serrations. *DPA4* expression domains overlap with those of the known leaf shape regulator *CUP-SHAPED COTYLEDON 2* (*CUC2*) and we provide evidence that *DPA4* negatively regulates *CUC2* expression independently of *MIR164A*, an established regulator of *CUC2*. Taken together, the data suggest DPA4 as a newly identified player in the signalling network that controls leaf serrations in *Arabidopsis thaliana*.

KEY WORDS: Leaf serration development, Polycomb group, Auxin, CUP-SHAPED COTYLEDON 2, *Arabidopsis thaliana*

INTRODUCTION

Plant leaves have a major role in the photosynthetic supply of nutrients, gas exchange, the distribution of nutrients and water transport (Tsukaya, 2006). To optimise these functions in different habitats, plants need to adapt leaf positioning, size and shape (Hasson et al., 2010; Nicotra et al., 2011).

An important trait of leaf shape variation is the outline of the leaf margin, which can be smooth, serrated (toothed) or lobed. If the gaps between lobes reach the midvein, leaves are designated as compound leaves and the lobes are referred to as leaflets, which can reiterate a dissecting pattern. In the simple *Arabidopsis thaliana* (*Arabidopsis*) leaf, the degree of serration differs between accessions and is developmentally regulated: juvenile leaves are smooth and serration increases in later-produced leaves. Increased serration can be caused by an increased number of teeth or by an increased sinus (the region between the teeth) depth (Nikovics et al., 2006; Tsukaya, 2006).

Leaf serration formation is mechanistically related to leaf primordia formation in the shoot apical meristem (SAM) (Scarpella et al., 2010). The auxin efflux carrier PIN-FORMED 1 (PIN1) establishes local auxin maxima that direct the outgrowth of the serrations (Scarpella et al., 2006). Accordingly, loss of *PIN1* function results in smooth leaf margins (Hay and Tsiantis, 2006). It was shown that the transcription factor CUP-SHAPED COTYLEDON 2 (CUC2) facilitates the initiation of serrations by enabling PIN1 to reorientate within the membranes of margin cells to change the auxin flux from a leaf tip oriented flux into a segmented flux towards convergence points where the serrations develop (Bilsborough et al., 2011). Accordingly, *CUC2* is essential for the formation of leaf serrations (Nikovics et al., 2006; Hasson et al., 2011). *cuc2* mutants fail to initiate auxin convergence points at the leaf margin early in development and subsequently display a no longer discrete, but homogeneous, auxin distribution at their smooth leaf margins (Kawamura et al., 2010; Bilsborough et al., 2011; Hasson et al., 2011). Expression of *CUC2* is observed along the leaf margin prior to the actual outgrowth of the teeth, which occurs at points of local *CUC2* repression (Bilsborough et al., 2011). After the initiation of the teeth, *CUC2* expression persists at the sinus region, where it functions, together with the partially redundant gene *CUC3*, in the maintenance of serration outgrowth (Hasson et al., 2011). *CUC2* is post-transcriptionally downregulated in leaves by a microRNA (miRNA) encoded by the *MIR164A* locus. *mir164a* mutant plants display enhanced leaf serrations, whereas overexpression of *MIR164A* results in smooth leaf margins (Nikovics et al., 2006). In a feedback loop, auxin downregulates *CUC2* both transcriptionally and post-transcriptionally by activation of *MIR164A* (Bilsborough et al., 2011).

Chromatin-mediated gene repression through Polycomb group (PcG) proteins has an impact on leaf development (Katz et al., 2004). PcG proteins are structurally unrelated repressive proteins that assemble in several Polycomb repressive complexes (PRCs), and the components of PRCs are highly conserved in higher eukaryotes (Schwartz and Pirrotta, 2008). Genes to be repressed are methylated at lysine 27 of histone H3 (H3K27me3) by PRC2, and this mark is subsequently recognised by a chromodomain component of PRC1 (Kuzmichev et al., 2005; Schwartz and Pirrotta, 2008). PRC1 stays associated with the repressed locus and catalyses mono-ubiquitylation of lysine 119 in histone H2A (H2AK119ub1), leading to a compaction of chromatin that represses transcription (Morey and Helin, 2010). In plants, PRC2 is conserved and was shown to be involved in deposition of the H3K27me3 mark (Pien and Grossniklaus, 2007). The catalytic core of the sporophytic PRC2 comprises one of the partially redundant

[1]Department of Plant Developmental Biology, [2]Plant Computational Biology, [3]Max Planck Genome Centre Cologne, Max Planck Institute for Plant Breeding Research, Carl von Linné Weg 10, 50829 Köln, Germany.

*Author for correspondence (turck@mpipz.mpg.de)

Accepted 3 May 2012

SET domain proteins CURLY LEAF (CLF) and SWINGER (SWN). In the double mutant of *CLF* and *SWN*, cell differentiation is strongly disturbed, resulting in growth as a callus-like structure (Chanvivattana et al., 2004; Schubert et al., 2005).

During recent years, several components with PRC1 functions were identified in *Arabidopsis* (Kotake et al., 2003; Calonje et al., 2008; Bratzel et al., 2010). LIKE HETEROCHROMATIN PROTEIN 1 (LHP1) was shown to colocalise with H3K27me3 via recognition of the modification by its chromodomain (Turck et al., 2007; Zhang et al., 2007b). LHP1 is required for the repression of some PRC2 targets, such as *FLOWERING LOCUS T* (*FT*) and *AGAMOUS* (Kotake et al., 2003; Adrian et al., 2010).

Determination of H3K27me3 target genes (Turck et al., 2007; Zhang et al., 2007a; Lafos et al., 2011) has revealed several genes involved in leaf margin development, including *PIN1*, *CUC2* and *MIR164A*, suggesting that leaf margin development is regulated by PcG proteins at several levels of the regulatory network described above.

Here, we describe a new player in leaf margin shape regulation, which we identified via a reverse genetics screen based on PcG target genes.

MATERIALS AND METHODS

Plant material

Seeds of *mir164a-4* (GABI_867E03) (Nikovics et al., 2006) and T-DNA insertion lines for *DPA4* (At5g06250) (SALK_150707 and Salk_088181C) (Alonso et al., 2003) were obtained from the Nottingham Arabidopsis Stock Centre (NASC). Lines *clf-28* (SALK_139371) (Doyle and Amasino, 2009), *swn-7* (SALK_109121) and *clf-28/swn-7* (Lafos et al., 2011), *cuc2-1* (Aida et al., 1997), *DR5::GFP* (Benková et al., 2003), *CUC2::CUC2:VENUS* (Heisler et al., 2005) and *35S::LHP1:HA* in Landsberg *erecta* (L*er*) ecotype (Turck et al., 2007) were described previously. Sequencing of SALK_150707 revealed an insertion in the intron of At5g06250 for SALK_150707 (line was annotated in first exon). All further experiments were conducted using homozygous plants of Salk_088181C (*dpa4-1*) and SALK_150707 (*dpa4-2*). Genotyping primers are listed in supplementary material Table S4. *cuc2-1* was genotyped as described (Gómez-Mena and Sablowski, 2008).

Growth conditions

PcG mutants and plants for chromatin immunoprecipitation (ChIP) experiments were grown on germination medium (GM; half-strength Murashige and Skoog medium supplemented with 1% sucrose) in growth cabinets (Percival) in a controlled environment at 20°C in long days (LD) of 16 hours light and 8 hours darkness. All other plants were grown on soil in LD in a greenhouse at 20°C or for short days (SD) of 8 hours light and 16 hours darkness in growth cabinets at 20°C, 70% humidity. Prior to sowing, all seeds were stratified at 4°C for 4 days. Plant age is indicated as days after sowing. Unless indicated otherwise, plants were harvested at Zeitgeber (ZT) 4 hours. Plants grown on soil were cut above the soil for sampling; for seedlings/calli grown on plates, whole plants were harvested.

Generation of transgenic plants

The coding region of *DPA4* was amplified from *Arabidopsis* (Col-0) cDNA and cloned into the binary pAlligator2 vector (Bensmihen et al., 2004) using the Gateway cloning system according to the manufacturer's instructions (Invitrogen). With this vector, transgenic plants overexpressing *DPA4* in Col-0 wild type, *DR5::GFP* and *CUC2::CUC2:VENUS* plants were generated as described (Bensmihen et al., 2004). Only single T-DNA insertion lines were used for phenotypic characterisation. For *DR5::GFP* and *CUC2::CUC2:VENUS* analysis, transgenic lines with phenotypes resembling that of the *35S::DPA4-1* line where chosen.

Expression analysis

Samples named 'flowers' contained flowers from stage 14, and 'apex/inflorescence' (apex/infl.) samples contained main inflorescences including closed flowers. For 'apex' samples, all leaves larger than 5 mm and the roots were removed. About 2-5 mm of hypocotyls remained in the sample. For 'leaf' samples, the leaves removed for 'apex' samples were collected. This results in apex- or leaf-enriched samples, but samples do not contain exclusively the respective tissue. Total RNA was isolated and transcribed into cDNA as described (Adrian et al., 2010). Quantitative real-time PCR (qRT-PCR) was performed using a BioRad iCycler iQ5 Real-Time PCR Detection System with EvaGreen dye (Biotium) to detect the product. Primer sequences are listed in supplementary material Table S4. *PP2AA3* (At1g13320) was used as reference gene (Martin-Tryon et al., 2007).

Genome-wide expression data were obtained using the AGRONOMICS1 Tiling Array (Affymetrix) (Rehrauer et al., 2010). Three biological replicates were processed for each genotype. cRNA synthesis and array hybridisation were performed as described (Rehrauer et al., 2010).

The aroma.affymetrix package (Bengtsson et al., 2008) together with the scripts agronomicsTools01.r were used to perform RMA normalisation and calculation of mean values over all probes per gene in R. To assign probes to genes, a CDF file was created according to aroma.affymetrix instructions using the AGRONOMICS1_At_TAIRG R package (Version 13.0.0, TAIR9 annotation) obtained from the Brainarray project webpage (Dai et al., 2005). Differentially expressed genes were determined using the Bioconductor (www.bioconductor.org) package RankProd (Hong et al., 2006). Genes with false discovery rate-corrected *P*-values below 0.05 were considered as differentially expressed. Data of this study are available at ArrayExpress (www.ebi.ac.uk/arrayexpress/) under accession number E-TABM-1195. To confirm the array results, we performed qRT-PCR and semi-quantitative RT-PCR on selected differentially expressed genes using biological replicates of the samples used for the array (supplementary material Fig. S7A,B).

In situ hybridisation

In situ hybridisation was performed as described (Bradley et al., 1993) with the modifications described (Jang et al., 2009). Templates for T7 RNA polymerase for probe labelling were created by PCR; for *CUC2* detection, a template created as described (Chandler et al., 2011) was used; the template for *DPA4* was amplified using the primers listed in supplementary material Table S4. The specificity of the *DPA4* probe (IS *DPA4*) was confirmed by the absence of signal in the *dpa4-2* mutant (supplementary material Fig. S9).

Identification of hexameric motifs in promoter regions

To find hexameric motifs in promoters the Motif Analysis tool from The Arabidopsis Information Resource (TAIR) was used (www.arabidopsis.org). The length of the upstream region considered for the analysis was 3000 bp.

Determination of PcG target genes

PcG target genes were determined by ChIP followed by hybridisation to whole genome tilling arrays (ChIP-chip) as described (Reimer and Turck, 2010; Göbel et al., 2010) in 10-day-old seedlings of *35S::LHP1:HA* (polyclonal anti-HA antibodies from rabbit; Sigma, H6908). Data analysis was performed using simple loess normalisation; LHP1 target genes were determined with the rank intersection method. Data from this study are available at ArrayExpress under accession number E-MTAB-749. The resulting list of LHP1 targets contains 5057 genes and is referred to here as 'PcG target genes', assuming colocalisation of LHP1 with the PcG-related histone mark H3K27me3 as shown previously (Turck et al., 2007; Zhang et al., 2007b). To confirm H3K27me3 abundance at the *DPA4* locus, ChIP was performed in 20-day-old seedlings as described (Farrona et al., 2011) (anti-H3K27me3 antibody; Millipore, 07-449).

Clustering and Gene Ontology (GO) analysis

PcG target genes were clustered according to expression in different developmental stages and organs using the Developmental Series from the AtGenExpress project (Schmid et al., 2005). After normalising expression values per gene by root mean square, hierarchical and k-means clustering were performed using Genesis software (Sturn et al., 2002) as described (Engelhorn and Turck, 2010). A hierarchical clustering analysis of a subset

of 500 randomly chosen H3K27me3 target genes revealed nine major branches, indicating nine groups of genes with similar expression patterns. Therefore, k=9 was used for the following k-means clustering analysis (supplementary material Fig. S10). One cluster (cluster 4) contained the group of mostly apex- and flower/floral organ-expressed genes. We used both gcRMA and MAS 5.0 normalised expression data and repeated the k-means clustering analysis ten times to obtain a final list of genes stably assigned to the apex cluster in all repetitions (105 genes). For functional enrichment analysis we used the web tool FatiGO (Al-Shahrour et al., 2007).

Scanning electron microscopy (SEM)

Fresh plant material was frozen in liquid nitrogen and remaining surface water was sublimed. Frozen samples were then spattered with platinum and transferred to the microscope under constant vacuum. Images were obtained using a Zeiss SUPRA 40VP scanning electron microscope including cryopreparation and transfer system (EMITECH K1250X).

Confocal microscopy

Images were taken using a TCS SP2 AOBS confocal laser-scanning microscope (Leica, Mannheim, Germany). Excitation was with an argon laser at 488 nm (GFP) or 514 nm (VENUS). Emission of GFP was detected from 492 to 550 nm and of VENUS from 518 to 575 nm. As a reference, the autofluorescence of chlorophyll was simultaneously detected between 650 and 730 nm. Images presented are average projections of 8-20 optical sections.

Quantification of leaf dissection index

To obtain silhouettes of leaves for figures and quantification, leaves were adhered to white paper and digitised using a scanner at 600 dpi resolution. Outlines of leaves were coloured in black and leaf surface was determined by counting of black pixels. Leaf perimeter was determined as the length of a closed path along all margin pixels. Leaf dissection index was calculated as (perimeter squared)/($4\pi \times$ area) as described (Bilsborough et al., 2011). All calculations and measurements were performed using a customised C++ program.

RESULTS

Identification of developmental regulators among PcG target genes

PcG target genes with tissue-specific expression were previously shown to play a major role in development according to Gene Ontology (GO) analysis (Zhang et al., 2007a). We generated genome-wide distribution data of the PcG protein LHP1 and classified target genes according to their expression pattern using publicly available expression data for different developmental stages and tissues and k-means clustering (supplementary material Fig. S10) (Schmid et al., 2005). A GO analysis for the 105 shoot apex-expressed LHP1 target genes revealed a significant over-representation of several developmental functions. This over-representation was only found for apex-expressed targets, not for all LHP1 targets or all apex-expressed genes (supplementary material Table S1). Since 50% of the genes in the apex cluster had not yet been characterised, we performed a screen for developmental abnormalities in T-DNA insertion lines that were likely loss-of-function alleles of these uncharacterised genes. We identified fourteen putative development-related PcG targets in the apex (DPAs). Here we report our characterisation of *DPA4* (At5g06250). Based on sequence similarity, DPA4 is a member of the B3 superfamily and a RAV [Related to ABSCISIC ACID-INSENSITIVE 3 (ABI3)/VIVIPAROUS1 (VP1)] transcriptional repressor containing the repressive motif described for B3 transcription factors (L/VRLFGV N/D M/L/V) in the variety VRLFGVNL (Romanel et al., 2009; Ikeda and Ohme-Takagi, 2009) (Fig. 1A,B).

DPA4 controls leaf margin outline and floral organ size

We analysed two independent T-DNA insertion lines in *DPA4* (*dpa4-1* and *dpa4-2*); both T-DNAs were inserted in the only intron of the gene but in opposite orientation (Fig. 1A). Expression of the full-length transcript was undetectable in *dpa4-2* and strongly reduced in *dpa4-1* (Fig. 1C).

Both *dpa4-1* and *dpa4-2* displayed enhanced leaf margin serration and elongated petals (Fig. 1D and supplementary material Fig. S1). No statistically significant difference in size was observed for other floral organs, although a tendency for bigger sepals in *dpa4-2* plants was observed. In accordance with the presence of residual full-length transcript in *dpa4-1*, serrations were stronger in *dpa4-2* than in *dpa4-1* (supplementary material Fig. S1A).

Serrations in *dpa4* plants were increased by a deepening of the sinuses and not by an increased number of serrations (supplementary material Fig. S1B,C). As in wild type, serrations were stronger in later-produced rosette leaves of *dpa4* plants, at which point the differences with wild type became more obvious (Fig. 1D). Rosette diameter and leaf surface were on average the same in *dpa4* and Col-0 plants (data not shown) and the shape of leaf epidermal cells was unchanged in *dpa4-2* plants (supplementary material Fig. S2). The leaf margin of *Arabidopsis thaliana* is characterised by highly elongated epidermal cells (Kawamura et al., 2010). Margin cells in *dpa4-1* plants appeared to elongate and develop normally, except for the increase in sinus depth and the associated more pronounced bending of the leaf margin cells (supplementary material Fig. S2C,D). Owing to the stronger deepening of serrations and absence of the full-length transcript, *dpa4-2* plants were used in all subsequent experiments.

Four independent *35S::DPA4* overexpressor lines [*35S::DPA4-1*, *35S::DPA4-2*, *35S::DPA4-8* (in *CUC2::CUC2:VENUS*) and *35S::DPA4-9* (in *DR5::GFP*)] developed narrow leaves without serrations (Fig. 1D and supplementary material Fig. S3A) and further lines displayed reduced serrations in several nuances, correlated with the amount of *DPA4* transcript (supplementary material Fig. S3B,C). The strongest lines, which did not show leaf serrations, could not be propagated as homozygotes. In each sowing, up to 20% of the plants were very small (~1.5 cm in diameter), produced progressively smaller leaves and died after several weeks, prior to flowering. These individuals expressed *DPA4* at approximately twice the level of their hemizygous siblings and were thus likely to be homozygous (supplementary material Fig. S3).

Hemizygous *35S::DPA4-1* and *35S::DPA4-2* plants produced more leaves prior to flowering than wild type and flowered at least 10 days later (Fig. 1D). In several transgenic lines, leaves of individual plants turned in a left-handed spiral (Fig. 1E). Additionally, these lines displayed several other abnormal phenotypes, such as a pronounced reduction in height, fasciation of inflorescences, reduced number of petals in some flowers and a broader replum resulting in abnormally shaped siliques (Fig. 1F-I).

DPA4 is expressed in organ boundaries and in the sinus of leaf serrations

We selected *DPA4* as a candidate for our screen because of its exclusive expression in the shoot apex and floral organs. Visualisation of the Developmental Series data with the Arabidopsis eFP browser (www.bar.utoronto.ca) showed strongest expression of *DPA4* in the inflorescence shoot apex and in siliques containing stage 3 seeds. Strong expression was also observed in transition/vegetative apices and flowers at stage 9. We confirmed

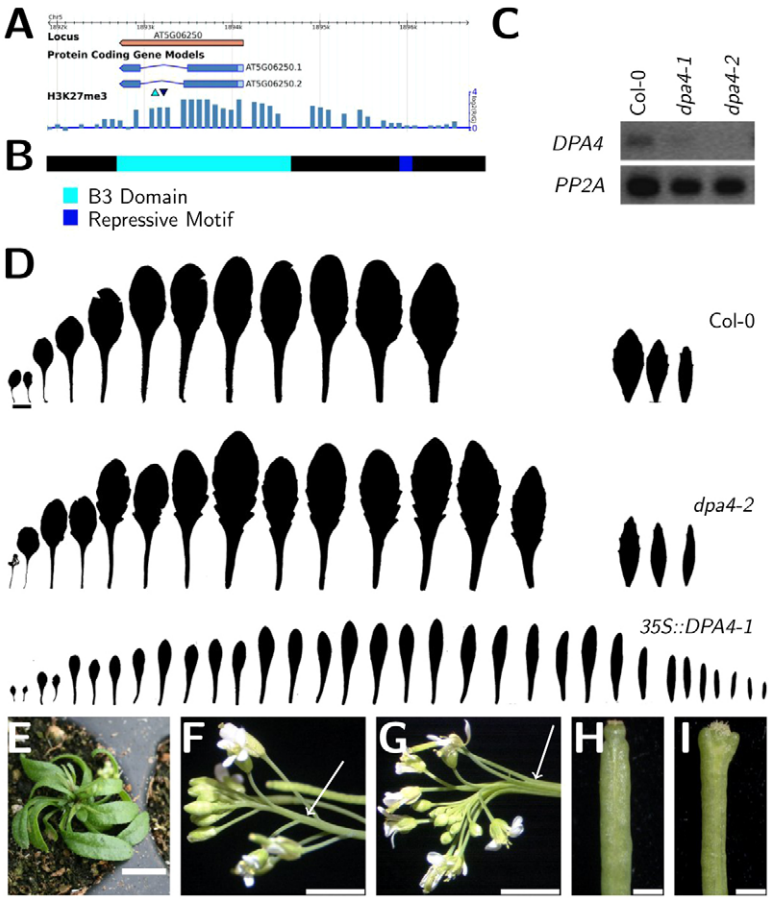

Fig. 1. Characteristics of *DPA4* and phenotype of *dpa4* and *35S::DPA4* plants. (**A**) *Arabidopsis thaliana DPA4* locus with associated gene models, T-DNA insertions used in this study (*dpa4-1*, light blue triangle; *dpa4-2*, dark blue triangle) and distribution of the histone mark H3K27me3 at the locus (Göbel et al., 2010). (**B**) Primary structure of DPA4 encoded by representative gene model At5g06250.2. The predicted protein contains the B3 domain (Pfam:PF02362) variety found in RAV transcription factors (Romanel et al., 2009) and the repressive motif L/V RLFGV N/D M/L/V (Ikeda and Ohme-Takagi, 2009). (**C**) Amplification of *DPA4* coding region from cDNA of 11-day-old seedlings. (**D**) Leaf series of Col-0, *dpa4-2* and *35S::DPA4-1*; separated leaves on the right are cauline leaves. (**E**) Twisted rosette leaves in a 7-week-old *35S::DPA4-2* plant. (**F**,**G**) Inflorescence of 5.5-week-old Col-0 (F) and *35S::DPA4-1* (G) plants. (**H**,**I**) Detailed view of a silique of 5.5-week-old Col-0 (H) and *35S::DPA4-1* (I) plants. Light conditions: LD. Scale bars: 1 cm in D,E; 0.25 cm in F,G; 0.1 cm in H,I.

that *DPA4* expression is higher in apex-enriched samples than in the corresponding leaf samples collected at different stages (supplementary material Fig. S4). In situ hybridisation experiments showed that expression of *DPA4* within the shoot apex is tightly restricted to the areas of primordia formation. In vegetative and transition apices, expression was observed at the emerging boundary between the shoot apex and the leaf primordium. *DPA4* expression persisted in this area as the leaf developed (Fig. 2A,B). In inflorescence apices, *DPA4* was expressed in the boundary between the inflorescence meristem and the emerging flowers; in floral meristems, *DPA4* expression marked the boundaries between emerging floral organs (Fig. 2C,D). In flowers, *DPA4* expression persisted between organs, and also between the two fused carpels (Fig. 2E). Thus, *DPA4* is expressed wherever organs separate from the SAM or from each other. In addition, *DPA4* expression was observed in the leaf sinus, suggesting a role of *DPA4* during the early stages of organ initiation and during early development in young organs (Fig. 2F,G).

The *DPA4* expression level but not its tissue specificity is regulated via PcG proteins

The very restricted spatial expression pattern of *DPA4* in organ boundaries suggests a tight control of *DPA4* expression that might be conferred through chromatin-mediated gene repression by PcG proteins. We probed the expression of DPA4 in plants mutated in components of the PcG pathway. In the severe *clf/swn* double mutants, PcG-mediated repression is abolished in the developing seedling. *DPA4* was ~6-fold upregulated at 22 days in *clf/swn*, whereas upregulation at 11 days was much weaker (Fig. 3A). In the single *clf* mutant, *DPA4* expression was slightly lower than in wild type. This observation is in accordance with results from our previous studies, in which *DPA4* expression was, among ~500 other PcG target genes, slightly upregulated in *clf/swn* (1.23-fold) and slightly downregulated in *clf* (Farrona et al., 2011).

To further elucidate the possible regulation of *DPA4* by PcG proteins, we performed ChIP with an anti-H3K27me3 antibody followed by semi-quantitative PCR on the *DPA4* locus (supplementary material Fig. S5). Strong H3K27me3 signal was detected in wild-type and *clf* plants, whereas the chromatin mark was absent from *clf/swn*. These results are in accordance with the *DPA4* expression data in the mutants. Whereas *clf* plants develop relatively normally apart from an early flowering phenotype and an upward curling of leaves, *clf/swn* double mutants develop into callus-like structures after germination (Fig. 3B) (Schubert et al., 2005). At 22 days, the formation of ectopic tissue is already visible, whereas the 11-day-old seedlings contain mainly differentiated tissue. Thus, *DPA4* expression is elevated with the loss of differentiation, suggesting that the strict tissue-specific regulation of *DPA4* depends on organ differentiation and might be lost in *clf/swn*. However, in situ hybridisation revealed that expression of *DPA4* was still restricted to discrete clusters of few cells in *clf/swn* callus tissue, indicating that additional regulation, apart from PcG-mediated repression, is involved in the tight regulation of *DPA4* (Fig. 3B).

DPA4 influences later stages of leaf serration development

The expression of *DPA4* in the boundaries of initiating and developing organs does not answer the question of whether the gene controls development at early stages in the shoot apex or later

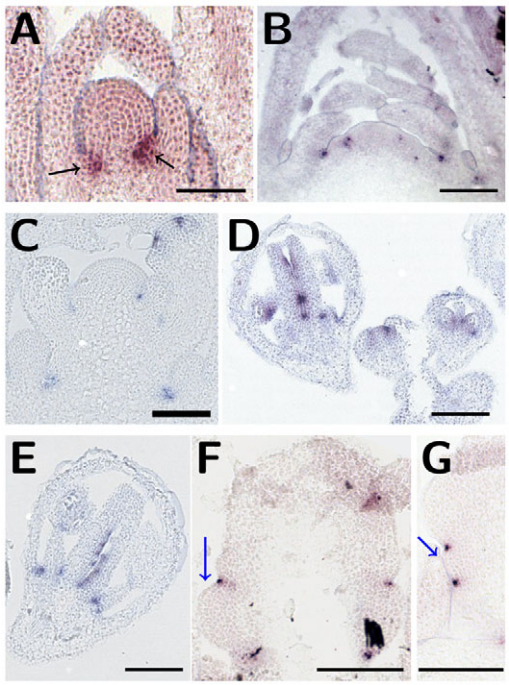

Fig. 2. Spatial expression pattern of *DPA4*. (**A**) Transition apex of 11-day-old plant in LD. (**B**) Vegetative apex of 35-day-old plant grown in SD. (**C**) Inflorescence apex of a plant that was shifted to LD for 7 days after 28 days in SD. (**D**) Various stages of young flowers of 28-day-old plant in LD. (**E**) Magnification of young flower. (**F**,**G**) Coronal sections through young leaves. Black arrows indicate *DPA4* expression foci and blue arrows indicate developing serrations. Scale bars: 25 μm in A; 100 μm in B-G.

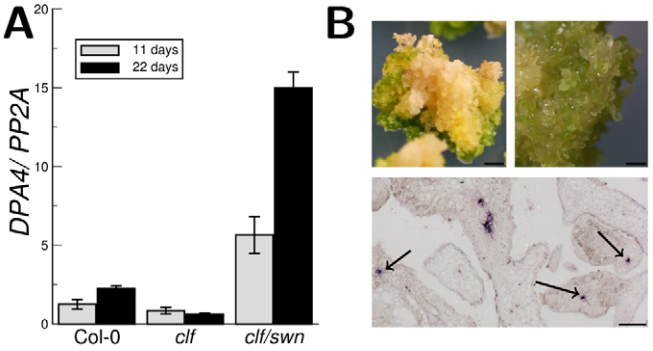

Fig. 3. Expression of *DPA4* in PcG mutants. (**A**) Expression of *DPA4* in whole seedling/callus tissue of *clf* and *clf/swn* grown in LD and harvested at ZT9. Data are based on a single experiment. Error bars indicate s.e.m. based on three technical replicates. Similar results were observed in a biological replicate (data not shown). (**B**) Upper panels show *clf/swn* callus grown for several weeks in LD. Lower panel shows expression pattern of *DPA4* in *clf/swn* callus tissue. Black arrows indicate some of the *DPA4* expression foci. Scale bars in B: 2 mm upper left; 0.4 mm upper right; 50 μm bottom.

in the developing organ. Defects in serration formation can be caused by a failure in serration initiation (as in *cuc2* mutants) or by defects in serration outgrowth (as in *cuc3* mutants) (Hasson et al., 2011). The deepened serrations observed in the mutants could be caused by an earlier onset of serration formation in developing leaves. However, no alterations during early serration initiation were observed in *dpa4* plants: serrations occurred at approximately the same leaf length in *dpa4* and Col-0 leaves (Fig. 4A,B). Therefore, the defects in *dpa4* plants originate later during the outgrowth of serrations. Differences to wild type only became apparent when the leaves reached a length of ~600 μm (supplementary material Fig. S6). We never observed serrations in homozygous plants of strong *35S::DPA4* lines, including at early stages of leaf serration development (Fig. 4C,D). Taken together, these observations suggest that *DPA4* can also prevent serration initiation if expressed ectopically, although its function in the accession Col-0 seems restricted to serration outgrowth.

Global expression profiling links DPA4 to auxin signalling

As a putative transcriptional repressor, DPA4 is expected to participate in leaf development by downregulating the transcription of target genes. Transcriptional profiling of *dpa4* and wild-type 'apex' tissue of 28-day-old plants grown in SD conditions identified 16 significantly upregulated and 61 downregulated genes in *dpa4* (supplementary material Table S2).

Functional characterisation of the differentially expressed genes provided no obvious candidates that might directly explain the leaf serration phenotype (supplementary material Fig. S7 and Table S3). The RAV B3 domain has been shown to recognise a CACCTG motif (Kagaya et al., 1999). Eight of the upregulated and 24 of the downregulated genes contain the CACCTG motif in their promoter region, which is not significantly different from the background distribution. Interestingly, the auxin-response element (AuxRE) TGTCTC, which is the binding motif for AUXIN RESPONSE FACTOR (ARF) family members (Ulmasov et al., 1999), was found in 57 of the 61 downregulated genes, which is a significant over-representation (P=0.00198 assuming binomial distribution). As the putative repressive function of DPA4 suggests that genes downregulated in *dpa4* plants are indirect targets of DPA4, an indirect regulation through ARF-mediated auxin signalling is more likely. The AuxRE was also found in 11 of the upregulated genes, but this does not constitute an over-representation of the motif.

Auxin distribution in *35S::DPA4* plants is similar to that in *cuc2-3* mutants

To test whether DPA4 affects auxin distribution, we analysed expression of the *DR5::GFP* auxin reporter in *35S::DPA4* plants (Benková et al., 2003). *35S::DPA4-9* plants showed GFP signal at the tip of initiating leaves, comparable to wild type, but failed to establish discrete auxin maxima at other positions, even at growth stages when wild-type leaves had already initiated serrations (Fig. 5A-D). At later stages, when serrations grew out in wild type, a diffuse expression of *DR5::GFP* was visible throughout the leaf margin of *35S::DPA4-9* plants (Fig. 5E,F). This auxin distribution pattern during leaf development resembles that observed in *cuc2* mutants (Bilsborough et al., 2011). *DPA4* and *CUC2* expression domains overlap in almost all post-embryonic parts of the plant. *CUC2*, as with *DPA4*, is expressed in the boundary region of the SAM, in leaf sinuses, at the base of emerging floral organs and the septum region of carpels (Fig. 2) (Ishida et al., 2000; Nikovics et al., 2006).

Alterations of *CUC2* transcript levels result in phenotypic changes that are similar to those observed in *dpa4* mutant plants, but the effects are opposite: expression of a miR164-resistant version of *CUC2* (*cuc2-1D*) results in enhanced leaf serration and enlarged leaf and petal size (Larue et al., 2009), similar to *dpa4* (Fig. 1C,D and supplementary material Fig. S1). By contrast,

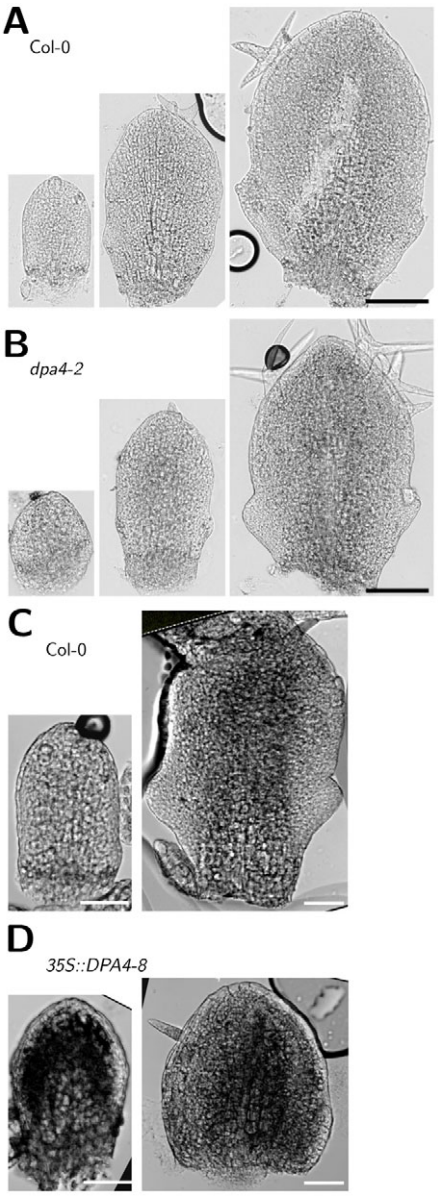

Fig. 4. Effect of *DPA4* during early stages of leaf development. (**A**,**B**) Leaves 6 to 8 of 13-day-old LD grown Col-0 (A) and *dpa4-2* (B) plants. (**C**,**D**) Leaves 5 and 6 of 12-day-old LD grown Col-0 (C) and *35S::DPA4-8* (D) plants. Scale bars: 100 μm in A,B; 50 μm in C,D.

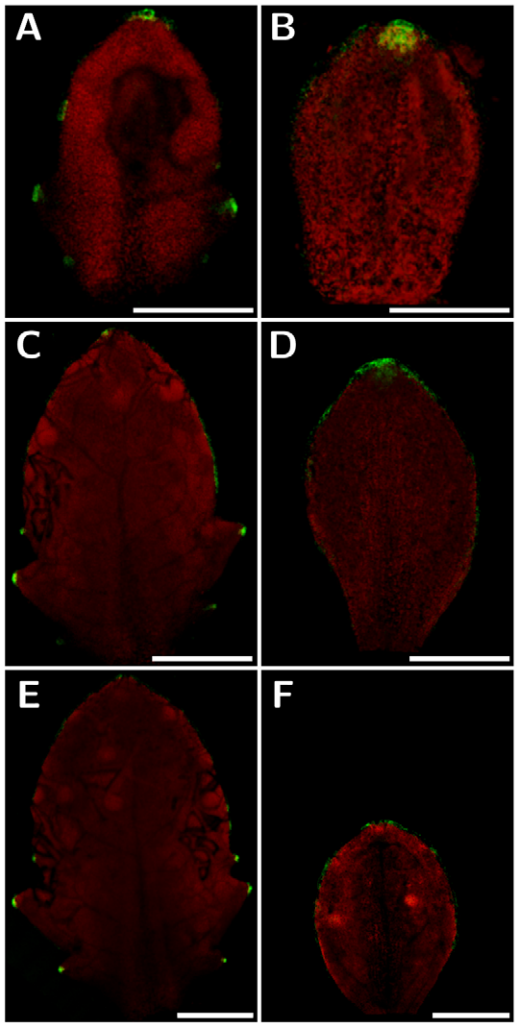

Fig. 5. *35S::DPA4* plants fail to initiate auxin activity maxima at the leaf margin. (**A-F**) Confocal micrographs of *DR5::GFP* expression in leaves 7 (A,B), 6 (C,D) and 5 (E,F) of 12-day-old Col-0 (A,C,E) and *35S::DPA4-9* (B,D,F) plants. Scale bars: 150 μm in A,B; 300 μm in C-F.

overexpression of *MIR164A* reduces *CUC2* levels and causes smooth leaf margins (Nikovics et al., 2006), as does overexpression of *DPA4*. Taken together, *DPA4* appears to act in the same process as *CUC2* but plays an antagonistic role.

Leaf shape regulation by DPA4 depends on *CUC2* but not *MIR164A*

To place *DPA4* within the genetic network for leaf serration development, we analysed the genetic interaction of *DPA4*, *CUC2* and *MIR164A*.

The alleles of *dpa4* and *cuc2-1* are in different genetic backgrounds, which show differences in leaf serration and leaf shape (*cuc2-1* in L*er*; *dpa4* in Col-0). We therefore scored several double-homozygous *cuc2-1/dpa4* F3 families for their degree of serration to account for phenotypic alterations caused by the genetic background. None of the *cuc2-1/dpa4* plants displayed any serrations, whereas serrations occurred in all single-homozygous *dpa4* families. In conclusion, serrations are abolished in *cuc2-1/dpa4* double mutants (Fig. 6A and supplementary material Fig. S8A,B). These results confirm the essential role of *CUC2* in serration formation, which was reported previously for the genetic interactions of *CUC2* and other leaf margin-controlling genes (Hasson et al., 2011).

Based on the epistatic relationship of their loss-of-function alleles and their antagonistic effect on leaf serration development, we expected *CUC2* to act downstream of *DPA4*. *CUC2* is directly repressed by miR164, and *DPA4* could antagonise *CUC2* by affecting this miRNA. We therefore tested whether the absence of *MIR164A* compromised the inhibitory effect of *DPA4* overexpression on leaf serration. All plants homozygous for *mir164a-4* carrying at least a hemizygous allele of *35S::DPA4* displayed a *35S::DPA4* phenotype (Fig. 6B), suggesting that the repression of leaf serrations by *DPA4* does not depend on miR164. Analysis of double *mir164a-4*/*dpa4* mutants confirmed that *DPA4* and miR164 act as independent antagonists of leaf serrations. The double *mir164a-4*/*dpa4* mutants displayed enhanced serrations

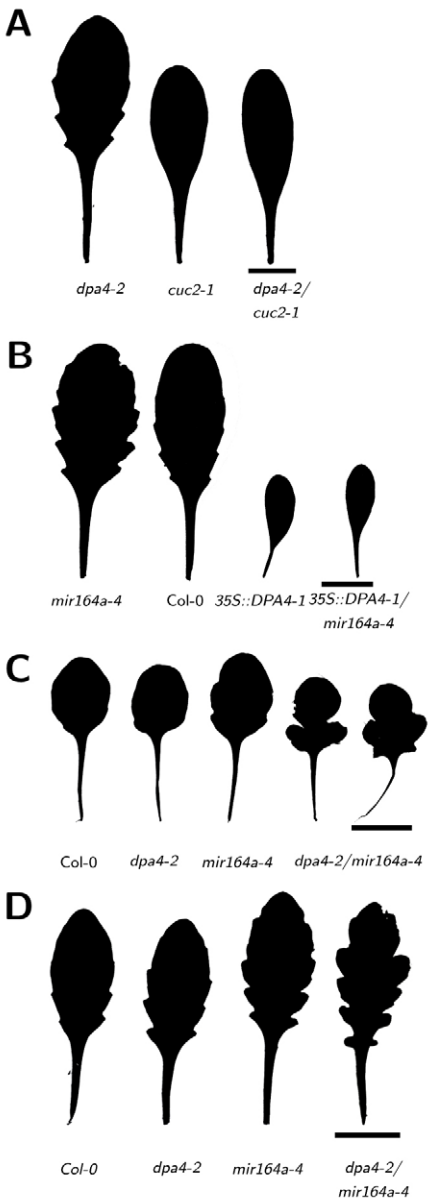

Fig. 6. Genetic interaction of *DPA4* with leaf development mutants. (**A**) Leaf shape of sixth true leaf of *dpa4-2*, *cuc2-1* homozygous plant that showed an otherwise Col-0-like phenotype and *dpa4-2/cuc2-1* double mutant. (**B**) Leaf shape of seventh true leaf of *mir164a-4*, Col-0, *35S::DPA4-1* and *35S::DPA4-1/mir164a-4* double mutant. (**C**) Leaf shape of fourth true leaf of Col-0, *dpa4-2*, *mir164a-4* and *dpa4-2/mir164a-4* double mutants. (**D**) Leaf shape of eighth true leaf of Col-0, *dpa4-2*, *mir164a-4* and *dpa4-2/mir164a-4* double mutants. Scale bars: 1 cm.

compared with either single mutant, indicating a parallel action of miR164 and *DPA4* (Fig. 6C,D and supplementary material Fig. S8C,D). The substantial increase in depth in the most basal serrations and juvenile leaves suggests an at least additive phenotype in the double *mir164a-4/dpa4* mutant.

DPA4 regulates *CUC2* expression

As a predicted transcriptional repressor, DPA4 could control leaf serration by modulating *CUC2* expression. Expression analysis in the single and double mutants of *MIR164A* and *DPA4* confirmed that *MIR164A* and *DPA4* have an additive effect on *CUC2* repression. Compared with Col-0, *CUC2* expression was increased to a similar degree in either single mutant, whereas an additive increase was observed in *mir164a-4/dpa4* double mutants (Fig. 7A). In addition, *CUC2* expression was strongly downregulated in *35S::DPA4-1* (Fig. 7B). This downregulation occurred in both the shoot apex and young developing leaves, where no *CUC2* transcript was detectable in *35S::DPA4* plants (Fig. 7C-G). *CUC2* is expressed in organ boundaries at the SAM and in sinuses of leaf serrations; therefore, the respective reduction and enhancement of these structures in *35S::DPA4* and *dpa4* plants could be the indirect cause of changes in *CUC2* expression levels. We used transgenic plants expressing a *CUC2::CUC2:VENUS* reporter construct (Heisler et al., 2005) to detect the impact of *DPA4* on *CUC2* expression prior to serration formation. As previously shown, *CUC2* is expressed in a slightly expanded region at the leaf base before leaf serration initiation and this pattern is gradually restricted to the sinuses of expanding serrations (Fig. 7D,F) (Bilsborough et al., 2011). In strong *DPA4*-overexpressing plants, no CUC2:VENUS signal was detected, suggesting that DPA4 mediates *CUC2* repression (Fig. 7E,G).

Taken together, our results establish *DPA4* as a new player in the genetic network of leaf margin regulation that represses leaf serration formation by negatively regulating the expression of *CUC2* in parallel to miR164 (Fig. 8).

DISCUSSION

DPA4 as repressor of leaf serrations

We identified *DPA4* as a gene with a role in development by a reverse genetics screen based on a rationally selected subset of genome-wide PcG target genes. The reduced number of candidate genes allowed screening for developmental abnormalities in several growth conditions. The relatively mild leaf serration phenotype in *dpa4* T-DNA insertion lines was best observed in SD growth conditions and could easily have been overlooked in a higher throughput approach. However, the role of *DPA4* in the regulation of leaf margin shape is clearly confirmed by the strong reciprocal enhancement of the single *mir164a* and *dpa4* phenotypes in combined double mutants (Fig. 6C,D).

Other lines of evidence indicate that DPA4 influences leaf serration by modulating *CUC2* transcript levels. First, leaf serrations are absent in *cuc2/dpa4* double mutants, indicating that *DPA4* requires a functional *CUC2* to increase leaf serrations (Fig. 6A). Furthermore, *CUC2* levels are upregulated in *dpa4* seedlings to levels similar to those observed in *mir164a* mutants (Fig. 7A). In addition, *CUC2* levels are strongly downregulated in *35S::DPA4* plants even before leaf serrations have initiated, which confirms that the reduced expression of *CUC2* is not only a consequence of the reduced number of serration sinuses, but is also more directly dependent on DPA4 (Fig. 7B-G). Nevertheless, it cannot be ruled out that *DPA4* also plays a role downstream of *CUC2*, and this will be subject to further studies.

The negative regulation of *CUC2* by *DPA4* is independent of miR164. First, the phenotype of *35S::DPA4* plants is not altered in the absence of *MIR164A*. In addition, the enhancement of leaf serrations in double *mir164a-4*/*dpa4* mutants is at least additive, as is the increase in *CUC2* expression. Thus, *DPA4* and *MIR164A* represent two parallel pathways that converge to fine-tune *CUC2* levels. Slight alterations in the expression of either gene might contribute to the plasticity of leaf serration development, such as the variation observed in serration depth in different culture conditions and variation dependent on

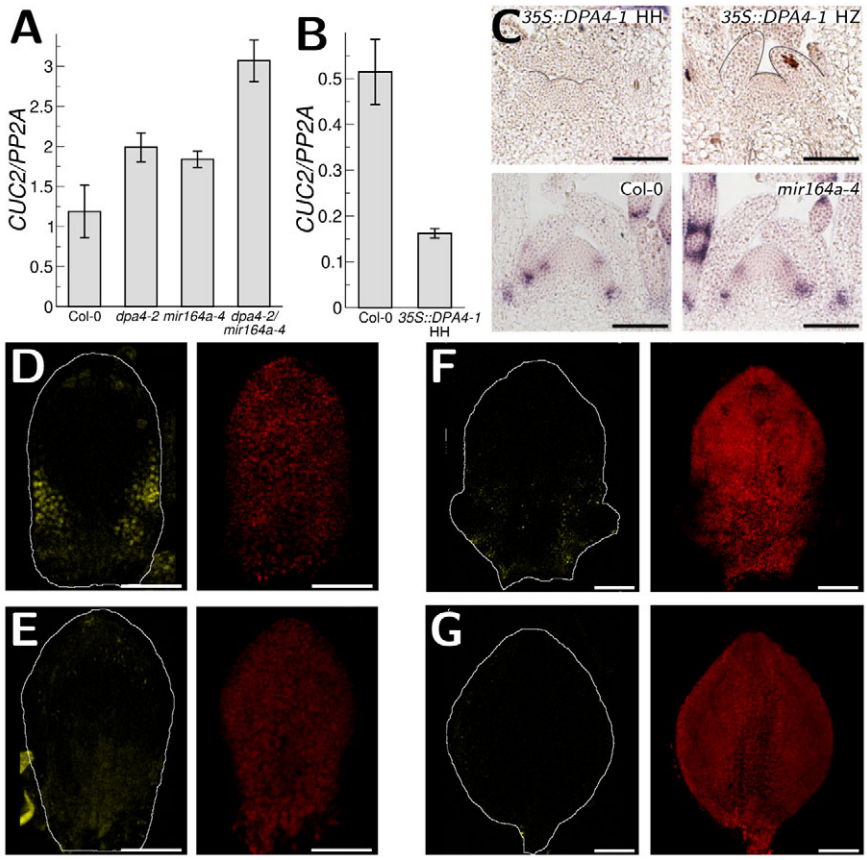

Fig. 7. Regulation of *CUC2* expression by *DPA4*. (**A**,**B**) Expression of *CUC2* in whole seedlings of 11-day-old plants grown in LD as measured by qRT-PCR. (A) Error bars indicate s.e.m. based on three biological replicates, each with three technical replicates. (B) Data are based on a single experiment; error bars indicate s.e.m. based on three technical replicates; similar results were observed in a biological replicate (data not shown). HH, putative homozygous *35S::DPA4-1* plants. (**C**) Spatial expression pattern of *CUC2* in apices of 4-week-old plants of the indicated genotype. HZ, hemizygous *35S::DPA4-1* plants based on size at harvesting. In upper panels the shoot apex and youngest pair of leaf primordia are outlined. (**D-G**) Confocal micrographs of *CUC2::CUC2:VENUS* expression in leaves 6 (D,E) and 5 (F,G) of 12-day-old Col-0 (D,F) and *35S::DPA4-8* (E,G) plants. Left, VENUS (yellow; leaf outlined); right, chlorophyll channel (red). Scale bars: 50 μm in C-E; 100 μm in F,G.

developmental age (Royer et al., 2009). In addition, the relative contribution of *DPA4* and *MIR164A* might be subject to natural variation. So far, a limited number of studies have reported quantitative trait loci (QTLs) for leaf serration depth in adult leaves, but apparently not just one but several major QTLs cause the variation between L*er* and Col and L*er* and Cape Verde Islands (Cvi) (Pérez-Pérez et al., 2002; Juenger et al., 2005; Pérez-Pérez et al., 2010).

Interestingly, the *dpa4-1* allele, which shows residual levels of *DPA4* transcript, has a milder effect on leaf serrations than the *dpa4-2* loss-of-function allele, suggesting a dosage dependency for *DPA4*. In this context it should be mentioned that *DPA4* might show redundancies with other closely related RAV transcription factors. The closest relative of *DPA4*, At3g11580, shows only 64% amino acid similarity and is predominantly expressed in mature seeds (Schmid et al., 2005). The T-DNA insertion lines available for At3g11580 did not generate loss-of-function alleles; therefore, the influence of redundancy has not yet been fully excluded in this study.

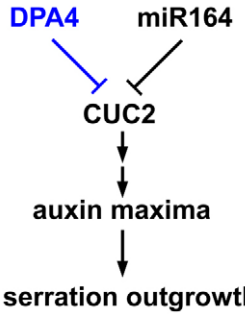

Fig. 8. Model for leaf serration formation. Leaf serrations are formed at auxin maxima (Scarpella et al., 2006), which are established by PIN1-mediated polar auxin transport (Hay et al., 2006). PIN1 localisation is regulated by *CUC2* (Bilsborough et al., 2011), which is repressed by miR164 (Nikovics et al., 2006). *DPA4* provides a second, negative, miR164-independent input for regulating *CUC2* expression. Interaction postulated during this study is shown in blue.

Severe developmental defects are observed in *35S::DPA4* plants that cannot be explained by a loss of *CUC2* function alone, suggesting that high-level ectopic expression of *DPA4* also affects other target genes. Indeed, we observed a strong downregulation of *CUC2*-related genes in *DPA4*-overexpressing plants (data not shown), but the direct involvement of *DPA4* is difficult to evaluate. *CUC3* expression is dependent on *CUC2*, which means that the loss of *CUC2* in *35S::DPA4* plants could be the primary cause of *CUC3* downregulation (Hasson et al., 2011). *CUC1* is expressed in boundary regions of the SAM, which is gradually consumed in *DPA4*-overexpressing plants (Fig. 7C). On the other hand, repression of additional CUC genes might lead to a gradual consumption of the meristematic cells and thus explain the smaller meristem size of *35S::DPA4* plants (Aida et al., 1997; Ishida et al., 2000). Future studies will have to clarify whether any of the CUC genes, including *CUC2*, are indeed direct targets of the supposed transcriptional repressor DPA4 or if other factors act as intermediates in the regulatory network.

PcG-mediated repression at several levels of leaf margin development

In addition to *DPA4*, the leaf shape-controlling factors *MIR164A*, *CUC2* and *PIN1* are PcG target genes. Given their network topology, it is not possible to conclude whether an upregulation of

these genes in *clf/swn* is immediately dependent on the loss of repressive chromatin or is indirectly mediated by alterations in expression within the network.

Expression of *DPA4* is restricted to defined areas in a few tissues. Interestingly, the putative target gene *CUC2* displays the same expression pattern, although *DPA4* is a negative regulator of *CUC2*. This indicates an as yet unknown regulatory mechanism that results in the co-expression of these genes, which then fine-tune their expression. PcG targets are on average more tissue specific than the remainder of the genome and several target genes display tissue-specific H3K27me3 labelling that is inversely correlated with their expression pattern (Zhang et al., 2007a; Lafos et al., 2011). This suggests that PcG-mediated regulation is responsible for the restricted expression pattern of *DPA4*, *CUC2* and *MIR164A* (this work) (Nikovics et al., 2006), although we found *DPA4* expression still restricted to discrete clusters of a few cells in the *clf/swn* callus tissue, suggesting that additional factors are responsible for the tissue-specific expression of *DPA4*. The preservation of tissue specificity in severe PcG mutants has also been observed for other H3K27me3 targets. In particular, *FT* expression is strictly dependent on the presence of a differentiated vasculature even in the absence of PcG-mediated repression (Farrona et al., 2011).

Little is known about *CUC2* upstream activators, which, given the similar expression pattern, could also contribute positively to the expression of *DPA4*. A recent report shows that SHOOT MERISTEMLESS (STM) acts as a direct activator of *CUC1* through CTGTCA elements found in the *CUC1* promoter (Spinelli et al., 2011). Prolonged ectopic expression of *STM* also leads to activation of *CUC2* and *MIR164A*, but this effect is indirect (Spinelli et al., 2011). All CUC genes and *DPA4* are expressed in a similar pattern in the SAM, but *CUC1* is not expressed in developing leaves. Chromatin remodelling ATPases are positive regulators of CUC genes, which are expressed at lower levels in plants that carry mutations in *BRAHMA* (*AtBRM*). *BRM* may participate in tissue-specific expression regulation, but its ubiquitous expression pattern suggests that at least one additional tissue-specific partner should be involved in the process (Kwon et al., 2006).

Complexity of the leaf serration gene network

DPA4 and *MIR164A* appear to play redundant roles in fine-tuning the expression of *CUC2* and show largely overlapping expression domains. The question arises as to why such redundant regulation has evolved or been maintained. *MIR164* and *DPA4* are both conserved in eudicots and the role of the *MIR164* and *CUC2* pathway in the evolution of leaf shape has been confirmed (Blein et al., 2008). The relative contribution of *DPA4* orthologues to leaf development in plant species that show more complicated leaf serration patterns than *Arabidopsis* remains to be seen.

It will be a challenge to integrate information on how developmental timing and the perception of environmental signals influence the expression of the single components in the gene network that controls leaf serration.

Acknowledgements

We thank E. Meyerowitz, D. Schubert and Q. Wang for provision of seeds; W. Werr for provision of a *CUC2* probe template and seeds; R. Franzen and E. Schmelzer for assistance with microscopy; V. Strizhova and L. Stephan for excellent technical assistance; and C. Vincent for sharing expertise of in situ hybridisation.

Funding

We thank the ERA-NET Plant Genomics [Deutsche Forschungsgemeinschaft (DFG)] and the Max Planck Society for funding. Deposited in PMC for immediate release.

Competing interests statement

The authors declare no competing financial interests.

Supplementary material

Supplementary material available online at
http://dev.biologists.org/lookup/suppl/doi:10.1242/dev.078618/-/DC1

References

Adrian, J., Farrona, S., Reimer, J. J., Albani, M. C., Coupland, G. and Turck, F. (2010). cis-Regulatory elements and chromatin state coordinately control temporal and spatial expression of FLOWERING LOCUS T in Arabidopsis. *Plant Cell* **22**, 1425-1440.

Aida, M., Ishida, T., Fukaki, H., Fujisawa, H. and Tasaka, M. (1997). Genes involved in organ separation in Arabidopsis: an analysis of the cup-shaped cotyledon mutant. *Plant Cell* **9**, 841-857.

Al-Shahrour, F., Minguez, P., Tárraga, J., Medina, I., Alloza, E., Montaner, D. and Dopazo, J. (2007). FatiGO +: a functional profiling tool for genomic data. Integration of functional annotation, regulatory motifs and interaction data with microarray experiments. *Nucleic Acids Res.* **35**, W91-W96.

Alonso, J. M., Stepanova, A. N., Leisse, T. J., Kim, C. J., Chen, H., Shinn, P., Stevenson, D. K., Zimmerman, J., Barajas, P., Cheuk, R. et al. (2003). Genome-wide insertional mutagenesis of Arabidopsis thaliana. *Science* **301**, 653-657.

Bengtsson, H., Simpson, K., Bullard, J. and Hansen, K. (2008). aroma.affymetrix: A generic framework in R for analyzing small to very large Affymetrix data sets in bounded memory. Technical Report 745, Department of Statistics, University of California, Berkeley, USA.

Benková, E., Michniewicz, M., Sauer, M., Teichmann, T., Seifertová, D., Jürgens, G. and Friml, J. (2003). Local, efflux-dependent auxin gradients as a common module for plant organ formation. *Cell* **115**, 591-602.

Bensmihen, S., To, A., Lambert, G., Kroj, T., Giraudat, J. and Parcy, F. (2004). Analysis of an activated ABI5 allele using a new selection method for transgenic Arabidopsis seeds. *FEBS Lett.* **561**, 127-131.

Bilsborough, G. D., Runions, A., Barkoulas, M., Jenkins, H. W., Hasson, A., Galinha, C., Laufs, P., Hay, A., Prusinkiewicz, P. and Tsiantis, M. (2011). Model for the regulation of Arabidopsis thaliana leaf margin development. *Proc. Natl. Acad. Sci. USA* **108**, 3424-3429.

Blein, T., Pulido, A., Vialette-Guiraud, A., Nikovics, K., Morin, H., Hay, A., Johansen, I. E., Tsiantis, M. and Laufs, P. (2008). A conserved molecular framework for compound leaf development. *Science* **322**, 1835-1839.

Bradley, D., Carpenter, R., Sommer, H., Hartley, N. and Coen, E. (1993). Complementary floral homeotic phenotypes result from opposite orientations of a transposon at the plena locus of Antirrhinum. *Cell* **72**, 85-95.

Bratzel, F., López-Torrejón, G., Koch, M., Pozo, J. C. D. and Calonje, M. (2010). Keeping cell identity in Arabidopsis requires PRC1 RING-finger homologs that catalyze H2A monoubiquitination. *Curr. Biol.* **20**, 1853-1859.

Calonje, M., Sanchez, R., Chen, L. and Sung, Z. R. (2008). EMBRYONIC FLOWER1 participates in polycomb group-mediated AG gene silencing in Arabidopsis. *Plant Cell* **20**, 277-291.

Cartagena, J. A., Matsunaga, S., Seki, M., Kurihara, D., Yokoyama, M., Shinozaki, K., Fujimoto, S., Azumi, Y., Uchiyama, S. and Fukui, K. (2008). The Arabidopsis SDG4 contributes to the regulation of pollen tube growth by methylation of histone H3 lysines 4 and 36 in mature pollen. *Dev. Biol.* **315**, 355-368.

Chandler, J. W., Cole, M., Jacobs, B., Comelli, P. and Werr, W. (2011). Genetic integration of DORNRÖSCHEN and DORNRÖSCHEN-LIKE reveals hierarchical interactions in auxin signalling and patterning of the Arabidopsis apical embryo. *Plant Mol. Biol.* **75**, 223-236.

Chanvivattana, Y., Bishopp, A., Schubert, D., Stock, C., Moon, Y.-H., Sung, Z. R. and Goodrich, J. (2004). Interaction of Polycomb-group proteins controlling flowering in Arabidopsis. *Development* **131**, 5263-5276.

Dai, M., Wang, P., Boyd, A. D., Kostov, G., Athey, B., Jones, E. G., Bunney, W. E., Myers, R. M., Speed, T. P., Akil, H. et al. (2005). Evolving gene/transcript definitions significantly alter the interpretation of GeneChip data. *Nucleic Acids Res.* **33**, e175.

Doyle, M. R. and Amasino, R. M. (2009). A single amino acid change in the enhancer of zeste ortholog CURLY LEAF results in vernalization-independent, rapid flowering in Arabidopsis. *Plant Physiol.* **151**, 1688-1697.

Engelhorn, J. and Turck, F. (2010). Metaanalysis of ChIP-chip data. *Methods Mol. Biol.* **631**, 185-207.

Farrona, S., Thorpe, F. L., Engelhorn, J., Adrian, J., Dong, X., Sarid-Krebs, L., Goodrich, J. and Turck, F. (2011). Tissue-specific expression of FLOWERING LOCUS T in Arabidopsis is maintained independently of polycomb group protein repression. *Plant Cell* **23**, 3204-3214.

Göbel, U., Reimer, J. and Turck, F. (2010). Genome-wide mapping of protein-DNA interaction by chromatin immunoprecipitation and DNA microarray hybridization (ChIP-chip). Part B: ChIP-chip data analysis. *Methods Mol. Biol.* **631**, 161-184.

Gómez-Mena, C. and Sablowski, R. (2008). ARABIDOPSIS THALIANA HOMEOBOX GENE1 establishes the basal boundaries of shoot organs and controls stem growth. *Plant Cell* **20**, 2059-2072.
Hasson, A., Blein, T. and Laufs, P. (2010). Leaving the meristem behind: the genetic and molecular control of leaf patterning and morphogenesis. *C. R. Biol.* **333**, 350-360.
Hasson, A., Plessis, A., Blein, T., Adroher, B., Grigg, S., Tsiantis, M., Boudaoud, A., Damerval, C. and Laufs, P. (2011). Evolution and diverse roles of the CUP-SHAPED COTYLEDON genes in Arabidopsis leaf development. *Plant Cell* **23**, 54-68.
Hay, A. and Tsiantis, M. (2006). The genetic basis for differences in leaf form between Arabidopsis thaliana and its wild relative Cardamine hirsuta. *Nat. Genet.* **38**, 942-947.
Hay, A., Barkoulas, M. and Tsiantis, M. (2006). ASYMMETRIC LEAVES1 and auxin activities converge to repress BREVIPEDICELLUS expression and promote leaf development in Arabidopsis. *Development* **133**, 3955-3961.
Heisler, M. G., Ohno, C., Das, P., Sieber, P., Reddy, G. V., Long, J. A. and Meyerowitz, E. M. (2005). Patterns of auxin transport and gene expression during primordium development revealed by live imaging of the Arabidopsis inflorescence meristem. *Curr. Biol.* **15**, 1899-1911.
Hong, F., Breitling, R., McEntee, C. W., Wittner, B. S., Nemhauser, J. L. and Chory, J. (2006). RankProd: a bioconductor package for detecting differentially expressed genes in meta-analysis. *Bioinformatics* **22**, 2825-2827.
Ikeda, M. and Ohme-Takagi, M. (2009). A novel group of transcriptional repressors in Arabidopsis. *Plant Cell Physiol.* **50**, 970-975.
Ishida, T., Aida, M., Takada, S. and Tasaka, M. (2000). Involvement of CUP-SHAPED COTYLEDON genes in gynoecium and ovule development in Arabidopsis thaliana. *Plant Cell Physiol.* **41**, 60-67.
Jagadeeswaran, G., Saini, A. and Sunkar, R. (2009). Biotic and abiotic stress down-regulate miR398 expression in Arabidopsis. *Planta* **229**, 1009-1014.
Jang, S., Torti, S. and Coupland, G. (2009). Genetic and spatial interactions between FT, TSF and SVP during the early stages of floral induction in Arabidopsis. *Plant J.* **60**, 614-625.
Juenger, T., Pérez-Pérez, J. M., Bernal, S. and Micol, J. L. (2005). Quantitative trait loci mapping of floral and leaf morphology traits in Arabidopsis thaliana: evidence for modular genetic architecture. *Evol. Dev.* **7**, 259-271.
Kagaya, Y., Ohmiya, K. and Hattori, T. (1999). RAV1, a novel DNA-binding protein, binds to bipartite recognition sequence through two distinct DNA-binding domains uniquely found in higher plants. *Nucleic Acids Res.* **27**, 470-478.
Katz, A., Oliva, M., Mosquna, A., Hakim, O. and Ohad, N. (2004). FIE and CURLY LEAF polycomb proteins interact in the regulation of homeobox gene expression during sporophyte development. *Plant J.* **37**, 707-719.
Kawamura, E., Horiguchi, G. and Tsukaya, H. (2010). Mechanisms of leaf tooth formation in Arabidopsis. *Plant J.* **62**, 429-441.
Kotake, T., Takada, S., Nakahigashi, K., Ohto, M. and Goto, K. (2003). Arabidopsis TERMINAL FLOWER 2 gene encodes a heterochromatin protein 1 homolog and represses both FLOWERING LOCUS T to regulate flowering time and several floral homeotic genes. *Plant Cell Physiol.* **44**, 555-564.
Kuusk, S., Sohlberg, J. J., Eklund, D. M. and Sundberg, E. (2006). Functionally redundant SHI family genes regulate Arabidopsis gynoecium development in a dose-dependent manner. *Plant J.* **47**, 99-111.
Kuzmichev, A., Margueron, R., Vaquero, A., Preissner, T. S., Scher, M., Kirmizis, A., Ouyang, X., Brockdorff, N., Abate-Shen, C., Farnham, P. and Reinberg, D. (2005). Composition and histone substrates of polycomb repressive group complexes change during cellular differentiation. *Proc. Natl. Acad. Sci. USA* **102**, 1859-1864.
Kwon, C. S., Hibara, K., Pfluger, J., Bezhani, S., Metha, H., Aida, M., Tasaka, M. and Wagner, D. (2006). A role for chromatin remodeling in regulation of CUC gene expression in the Arabidopsis cotyledon boundary. *Development* **133**, 3223-3230.
Lafos, M., Kroll, P., Hohenstatt, M. L., Thorpe, F. L., Clarenz, O. and Schubert, D. (2011). Dynamic regulation of H3K27 trimethylation during Arabidopsis differentiation. *PLoS Genet.* **7**, e1002040.
Larue, C. T., Wen, J. and Walker, J. C. (2009). A microRNA-transcription factor module regulates lateral organ size and patterning in Arabidopsis. *Plant J.* **58**, 450-463.
Mallory, A. C., Dugas, D. V., Bartel, D. P. and Bartel, B. (2004). MicroRNA regulation of NAC-domain targets is required for proper formation and separation of adjacent embryonic, vegetative, and floral organs. *Curr. Biol.* **14**, 1035-1046.
Martin-Tryon, E. L., Kreps, J. A. and Harmer, S. L. (2007). GIGANTEA acts in blue light signaling and has biochemically separable roles in circadian clock and flowering time regulation. *Plant Physiol.* **143**, 473-486.
Morey, L. and Helin, K. (2010). Polycomb group protein-mediated repression of transcription. *Trends Biochem. Sci.* **35**, 323-332.
Nicotra, A. B., Leigh, A., Boyce, C. K., Jones, C. S., Niklas, K. J., Royer, D. L. and Tsukaya, H. (2011). The evolution and functional significance of leaf shape in the angiosperms. *Func. Plant Biol.* **38**, 535-552.
Nikovics, K., Blein, T., Peaucelle, A., Ishida, T., Morin, H., Aida, M. and Laufs, P. (2006). The balance between the MIR164A and CUC2 genes controls leaf margin serration in Arabidopsis. *Plant Cell* **18**, 2929-2945.
Pérez-Pérez, J. M., Serrano-Cartagena, J. and Micol, J. L. (2002). Genetic analysis of natural variations in the architecture of Arabidopsis thaliana vegetative leaves. *Genetics* **162**, 893-915.
Pérez-Pérez, J. M., Esteve-Bruna, D. and Micol, J. L. (2010). QTL analysis of leaf architecture. *J. Plant Res.* **123**, 15-23.
Pien, S. and Grossniklaus, U. (2007). Polycomb group and trithorax group proteins in Arabidopsis. *Biochim. Biophys. Acta* **1769**, 375-382.
Rehrauer, H., Aquino, C., Gruissem, W., Henz, S. R., Hilson, P., Laubinger, S., Naouar, N., Patrignani, A., Rombauts, S., Shu et al. (2010). AGRONOMICS1: a new resource for Arabidopsis transcriptome profiling. *Plant Physiol.* **152**, 487-499.
Reimer, J. J. and Turck, F. (2010). Genome-wide mapping of protein-DNA interaction by chromatin immunoprecipitation and DNA microarray hybridization (ChIP-chip). Part A: ChIP-chip molecular methods. *Methods Mol. Biol.* **631**, 139-160.
Romanel, E. A. C., Schrago, C. G., Counago, R. M., Russo, C. A. M. and Alves-Ferreira, M. (2009). Evolution of the B3 DNA binding superfamily: new insights into REM family gene diversification. *PLoS ONE* **4**, e5791.
Royer, D. L., Meyerson, L. A., Robertson, K. M. and Adams, J. M. (2009). Phenotypic plasticity of leaf shape along a temperature gradient in Acer rubrum. *PLoS ONE* **4**, e7653.
Scarpella, E., Marcos, D., Friml, J. and Berleth, T. (2006). Control of leaf vascular patterning by polar auxin transport. *Genes Dev.* **20**, 1015-1027.
Scarpella, E., Barkoulas, M. and Tsiantis, M. (2010). Control of leaf and vein development by auxin. *Cold Spring Harb. Perspect. Biol.* **2**, a001511.
Schmid, M., Davison, T. S., Henz, S. R., Pape, U. J., Demar, M., Vingron, M., Schölkopf, B., Weigel, D. and Lohmann, J. U. (2005). A gene expression map of Arabidopsis thaliana development. *Nat. Genet.* **37**, 501-506.
Schubert, D., Clarenz, O. and Goodrich, J. (2005). Epigenetic control of plant development by Polycomb-group proteins. *Curr. Opin. Plant Biol.* **8**, 553-561.
Schwartz, Y. B. and Pirrotta, V. (2008). Polycomb complexes and epigenetic states. *Curr. Opin. Cell Biol.* **20**, 266-273.
Spinelli, S. V., Martin, A. P., Viola, I. L., Gonzalez, D. H. and Palatnik, J. F. (2011). A mechanistic link between STM and CUC1 during Arabidopsis development. *Plant Physiol.* **156**, 1894-1904.
Sturn, A., Quackenbush, J. and Trajanoski, Z. (2002). Genesis: cluster analysis of microarray data. *Bioinformatics* **18**, 207-208.
Tsukaya, H. (2006). Mechanism of leaf-shape determination. *Annu. Rev. Plant Biol.* **57**, 477-496.
Turck, F., Roudier, F., Farrona, S., Martin-Magniette, M.-L., Guillaume, E., Buisine, N., Gagnot, S., Martienssen, R. A., Coupland, G. and Colot, V. (2007). Arabidopsis TFL2/LHP1 specifically associates with genes marked by trimethylation of histone H3 lysine 27. *PLoS Genet.* **3**, e86.
Ulmasov, T., Hagen, G. and Guilfoyle, T. J. (1999). Activation and repression of transcription by auxin-response factors. *Proc. Natl. Acad. Sci. USA* **96**, 5844-5849.
Zhang, X., Clarenz, O., Cokus, S., Bernatavichute, Y. V., Pellegrini, M., Goodrich, J. and Jacobsen, S. E. (2007a). Whole-genome analysis of histone H3 lysine 27 trimethylation in Arabidopsis. *PLoS Biol.* **5**, e129.
Zhang, X., Germann, S., Blus, B. J., Khorasanizadeh, S., Gaudin, V. and Jacobsen, S. E. (2007b). The Arabidopsis LHP1 protein colocalizes with histone H3 Lys27 trimethylation. *Nat. Struct. Mol. Biol.* **14**, 869-871.